Formation of a molecular Bose-Einstein condensate and an entangled atomic gas by Feshbach resonance

V. A. Yurovsky and A. Ben-Reuven
School of Chemistry, Tel Aviv University, 69978 Tel Aviv, Israel
(Received 13 May 2002; revised manuscript received 30 January 2003; published 23 April 2003)

Association in an atomic Bose-Einstein condensate, and dissociation of the resulting molecular condensate, due to a Feshbach resonance in a time-dependent magnetic field, are analyzed incorporating non-mean-field quantum corrections and inelastic collisions. Calculations for the Na atomic condensate demonstrate that there exist optimal conditions under which about 80% of the atomic population can be converted to a relatively long-lived molecular condensate (with lifetimes of 100 ms and more). Entangled atoms in two-mode squeezed states (with noise reduction of about 30 dB) may also be formed by molecular dissociation.

DOI: 10.1103/PhysRevA.67.043611 PACS number(s): 03.75.Gg, 03.75.Mn, 42.50.Dv, 82.20.Xr

INTRODUCTION

The recently discovered Bose-Einstein condensates (BEC), or matter waves, resemble in certain ways coherent electromagnetic radiation. This similarity stimulated the development of atom optics [1], involving nonclassical states of the atomic fields, such as squeezed and entangled states [2]. Squeezed states are characterized by noise reduction, and can be applied in communications and measurements. Entangled states of a decomposable system cannot be expressed as a product of the component states, and can be used in quantum computing and communications. Squeezed atomic states can be formed in four-wave mixing [3], in arrays of atomic traps [4], in multimode condensates [5,6], in the decay of unstable BEC [7], in collisions of BEC wavepackets [7], and as the outcome of Bogoliubov fluctuations subject to stimulated light scattering [8] or Beliaev damping [9]. The squeezing can be measured experimentally by using homodyne detection, analogous to the one used in quantum optics (see, Ref. [2]). The key component of this method—a beam splitter—already exists (see, Ref. [10]).

The present work suggests the dissociation of molecular BEC as a source of atom pairs in two-mode squeezed states that are entangled. The formation of single-mode squeezed states by the same mechanism has been discussed in Refs. [11–13]. The formation of entangled atomic pairs in the dissociation of individual diatomic molecules has been considered in Ref. [14]. Other mechanisms of formation of entangled gases have been discussed in Refs. [5,7,8].

The molecular BEC required as the source of the entangled gas is interesting in its own right, although its effective production has not been achieved yet. The formation of a molecular BEC by direct cooling of molecular gases is obstructed by the rotational degrees of freedom. An alternative method is the association of atomic BEC [15,16]. A Raman process of photoassociation [15], realized experimentally [17], was not sufficiently productive because of spontaneous emission [18]. We consider here the association of atoms in a BEC by Feshbach resonance [16] in a time-dependent magnetic field. Such a process is associated with the large condensate loss observed in experiments [19]. This loss follows from the deactivation of resonant molecules in excited states by inelastic collisions [20,21,16], as well as from the formation of noncondensate atoms by molecular dissociation.

Reference [22] treats the condensate loss as a dissociation of single molecules. Many-body effects have been incorporated in Ref. [21] by introducing a width to the molecular condensate state. A more rigorous analysis has been performed in Refs. [23,24]. In that analysis, equations for the atomic and molecular mean fields were complemented by equations for the normal and anomalous densities of atomic fluctuations, allowing the study of quantum properties of the atomic states formed by molecular dissociation. These properties have been analyzed numerically by using a positive-P representation in Refs. [11,25]. Some qualitative results related to the quantum properties have been also presented in Ref. [26]. An exact solution for the case of a single atomic mode has been obtained in Ref. [27]. The approaches of Refs. [11,23–27] did not take into account the deactivating collisions, unlike the present analysis and Refs. [20,21]. We generalize here the parametric approximation used in Refs. [12,13]. Preliminary results of the present paper have been reported in Ref. [28].

An advantage of the use of Feshbach association is the possibility of reducing the negative effect of collisions by lowering the condensate density. We show here that the molecular condensate produced by this method can survive, under favorable conditions, over extended time intervals. Other impressive outcomes of the present approach are the extent of (near-total) conversion to entangled atoms or a molecular condensate, as well as the extreme degree of squeezing and the relatively long molecular BEC lifetimes achievable.

I. THE MODEL

Our model is based on the Hamiltonian used in Refs. [20,21] in a mean-field description of the coupled atomic and molecular fields. This treatment is improved here by the use of a generalized parametric approximation in order to incorporate various effects. The word ''parametric'' refers to the treatment of the atomic field in a fully second-quantized form. The word ''generalized'' refers to an improvement on a version of the parametric approximation [7,13] in which the time dependence of the molecular field and the effect of de-

activating collisions were not incorporated.

The Hamiltonian of Refs. [20,21] can be expressed in the momentum representation in terms of the annihilation operators of the atomic and molecular fields involved, $\hat{\Psi}_a(\mathbf{p},t)$ and $\hat{\Psi}_\alpha(\mathbf{p},t)$, respectively. Using units with $\hbar=1$, the Hamiltonian is

$$\hat{H}=\int d^3p\left\{\left[\frac{p^2}{2m}+\epsilon_a(t)\right]\hat{\Psi}_a^\dagger(\mathbf{p},t)\hat{\Psi}_a(\mathbf{p},t) + \sum_{\alpha=m,u,d}\left[\frac{p^2}{4m}-E_\alpha\right]\hat{\Psi}_\alpha^\dagger(\mathbf{p},t)\hat{\Psi}_\alpha(\mathbf{p},t)\right\}+\hat{V}_h+\hat{V}_h^\dagger + \sum_d(\hat{V}_d+\hat{V}_d^\dagger)+\sum_{u,d}(\hat{V}_{ud}+\hat{V}_{ud}^\dagger), \tag{1}$$

where m is the atomic mass, $\epsilon_a(t)=-\frac{1}{2}\mu[B(t)-B_0]$ is the time-dependent Zeeman shift of the atom in an external magnetic field $B(t)$ relative to half the energy of the molecular state (which is fixed as the zero energy point), μ is the difference between the magnetic momenta of an atomic pair and a molecule, and B_0 is the resonance value of B. The subscript α describes the various molecular states, with $\alpha=m$ denoting the resonance state and $\alpha=u,d$ denoting the ''dump'' states above and below the resonance state, respectively. The Zeeman shift of the dump states is negligibly small compared to the energies of transitions E_α from the resonance state (i.e., $E_m=0$, $E_u<0$, $E_d>0$).

The Feshbach coupling of the atomic and molecular fields, described by

$$\hat{V}_h=(2\pi)^{-3/2}\int d^3p\,d^3p'\,V_h(\mathbf{p}-\mathbf{p}') \times\hat{\Psi}_m^\dagger(\mathbf{p}+\mathbf{p}',t)\hat{\Psi}_a(\mathbf{p},t)\hat{\Psi}_a(\mathbf{p}',t), \tag{2}$$

contains a product of two atomic creation operators and, therefore, describes the formation of entangled atomic pairs, in analogy with parametric down-conversion in quantum optics (see, Ref. [2]). The momentum dependence of V_h is necessary to avoid divergences in subsequent calculations (see, also Ref. [23]). Only its maximal value $V_h(0)=g$ has a physical meaning, being related to the phenomenological resonance strength Δ as

$$|g|^2=2\pi|a_a|\mu\Delta/m, \tag{3}$$

where a_a is the elastic-scattering length. The terms

$$\hat{V}_d=(2\pi)^{-3/2}\int d^3p'\,d^3p_d\,d^3p_m\,d_d(\mathbf{p}_d-2\mathbf{p}')\hat{\Psi}_d^\dagger(\mathbf{p}',t) \times\hat{\Psi}_d^\dagger(\mathbf{p}_d,t)\hat{\Psi}_m(\mathbf{p}_m,t)\hat{\Psi}_a(\mathbf{p}'+\mathbf{p}_d-\mathbf{p}_m,t) \tag{4}$$

describe the deactivating collisions of the resonant molecules with atoms

$$A_2(m)+A(\text{cold})\rightarrow A_2(d)+A(\text{hot}). \tag{5}$$

The inelastic collisions between the resonant molecules

$$A_2(m)+A_2(m)\rightarrow A_2(d)+A_2(u) \tag{6}$$

are described by

$$\hat{V}_{ud}=(2\pi)^{-3/2}\int d^3p_m\,d^3p_d\,d^3p_u\,d_{ud}(\mathbf{p}_u-\mathbf{p}_d)\hat{\Psi}_u^\dagger(\mathbf{p}_u,t) \times\hat{\Psi}_d^\dagger(\mathbf{p}_d,t)\hat{\Psi}_m(\mathbf{p}_m,t)\hat{\Psi}_m(\mathbf{p}_u+\mathbf{p}_d-\mathbf{p}_m,t). \tag{7}$$

Spatial inhomogeneity due to the trapping potential and elastic collisions can be neglected here (see discussion below in Sec. III).

Let the initial state of the atomic field at $t=t_0$ be a coherent state of zero kinetic energy

$$\hat{\Psi}_a(\mathbf{p},t_0)|\text{in}\rangle=(2\pi)^{3/2}\varphi_0\delta(\mathbf{p})|\text{in}\rangle, \tag{8}$$

where $|\varphi_0|^2=n_a(t_0)$ is the initial atomic density and $|\text{in}\rangle$ is the time-independent state vector in the Heisenberg representation. A pair of condensate atoms forms a molecule of zero kinetic energy. Therefore, the resonant molecules can be represented by a mean field $\varphi_m(t)$ as

$$\langle\text{in}|\hat{\Psi}_m(\mathbf{p},t)|\text{in}\rangle=(2\pi)^{3/2}\varphi_m(t)\,\delta(\mathbf{p}), \tag{9}$$

where $|\varphi_m(t)|^2=n_m(t)$ is the molecular condensate density. This approach therefore takes into account the time dependence of the molecular mean field, but neglects fluctuations of the molecular field due to Feshbach coupling of noncondensate atoms.

The outcome of atom-molecule and molecule-molecule deactivating collisions is introduced, as in Refs. [20,21], by adding the molecular dump states. The elimination of these states in a second-quantized description should, however, be done in a different way (see Appendix A). In the Markovian approximation, the equation of motion for the atomic field attains the form

$$i\dot{\hat{\Psi}}_a(\mathbf{p},t)=\left[\frac{p^2}{2m}+\epsilon_a(t)-i\gamma|\varphi_m(t)|^2\right]\hat{\Psi}_a(\mathbf{p},t) +2g^*\varphi_m(t)\hat{\Psi}_a^\dagger(-\mathbf{p},t)+i\hat{F}(\mathbf{p},t), \tag{10}$$

where $V_h(p)$ is replaced by its maximal value $V_h(0)=g$ [see Eq. (3)]. The parameter γ describes the width of atomic states due to deactivating collisions (5) (see Refs. [20,21]). The corresponding shift can be neglected compared to other energy scales in real physical situations. The quantum noise source $\hat{F}(\mathbf{p},t)$ is δ-correlated in the Markovian approximation, obeying

$$\langle\text{in}|[\hat{F}(\mathbf{p},t),\hat{F}^\dagger(\mathbf{p}',t')]|\text{in}\rangle=2\gamma|\varphi_m(t)|^2\delta(t-t')\,\delta(\mathbf{p}-\mathbf{p}'). \tag{11}$$

In the generalized parametric approximation, the atomic-field operator is represented in the form

$$\hat{\Psi}_a(\mathbf{p},t)=[\hat{A}(\mathbf{p},t)\psi_c(p,t)+\hat{A}^\dagger(-\mathbf{p},t)\psi_s(p,t)]C(t), \tag{12}$$

where

$$C(t)=\exp\left(-\int_{t_0}^{t}dt_1\gamma|\varphi_m(t_1)|^2\right). \tag{13}$$

The operators $\hat{A}(\mathbf{p},t)$ are expressible in terms of $\hat{\Psi}_a(\mathbf{p},t_0)$, $\hat{F}(\mathbf{p},t)$, and the c-number solutions $\psi_{c,s}(p,t)$ of the equations

$$i\dot{\psi}_{c,s}(p,t)=\left[\frac{p^2}{2m}+\epsilon_a(t)\right]\psi_{c,s}(p,t)+2g^*\varphi_m(t)\psi^*_{s,c}(p,t), \tag{14}$$

given the initial conditions $\psi_c(p,t_0)=1$ and $\psi_s(p,t_0)=0$ (see Appendix B).

The atomic density

$$n_a(t)=(2\pi)^{-3}\int d^3p_1d^3p_2\exp[i(\mathbf{p}_2-\mathbf{p}_1)\cdot\mathbf{r}]$$
$$\times\langle \mathrm{in}|\hat{\Psi}^\dagger_a(\mathbf{p}_1,t)\hat{\Psi}_a(\mathbf{p}_2,t)|\mathrm{in}\rangle \tag{15}$$

then appears to be $\mathbf{r}$ independent, and comprises the sum $n_a(t)=n_0(t)+n_s(t)$ of the densities of condensate atoms $n_0(t)=|\langle \mathrm{in}|\hat{\Psi}_a(0,t)|\mathrm{in}\rangle|^2$ [see Eq. (B6)], and of noncondensate (entangled) atoms $n_s(t)$ in a wide spectrum of kinetic energies $E=p^2/(2m)$,

$$n_s(t)=\int dE\tilde{n}_s(E,t), \tag{16}$$

where the energy spectrum $\tilde{n}_s(E,t)$ is related to the momentum spectrum $n_s(p,t)$ [see Eq. (B7)] as

$$\tilde{n}_s(E,t)=\frac{mp}{2\pi^2}n_s(p,t). \tag{17}$$

The equation of motion for the molecular mean field $\varphi_m(t)$ is obtained by a similar elimination of the dump fields from the corresponding operator equation, followed by a mean-field averaging. We thus obtain

$$i\dot{\varphi}_m(t)=gm_0(t)+\frac{1}{2\pi^2}\int_0^\infty p^2dpV_h(p)m_s(p,t)-i(\gamma n_a(t)$$
$$+\gamma_m|\varphi_m(t)|^2)\varphi_m(t), \tag{18}$$

where the parameter γ_m describes molecule-molecule deactivation collisions (see Refs. [20,21]), and the anomalous densities of the condensate and noncondensate atoms $m_0(t)$ and $m_s(p,t)$ are defined by Eq. (B8). A numerical solution of Eqs. (14) on a grid of values of p, combined with Eq. (18), is consistently sufficient for elucidating the dynamics of the system. The atomic energy was renormalized in the same manner as in Ref. [23].

The present approach becomes mathematically equivalent to the approach of Ref. [23] if the inelastic collisions are neglected (justifiably in the case of ^{85}Rb experiment [29]). At a low-molecular density, the effect of noncondensate atoms is equivalent to the contribution to the width of the molecular state made in Ref. [21] for the same process (see Appendix C).

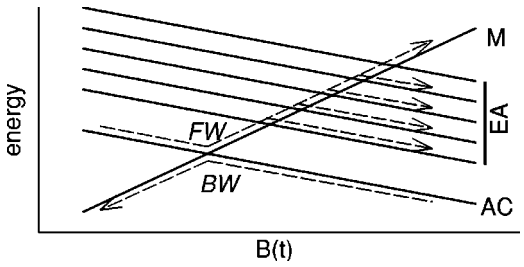

FIG. 1. Schematic illustration of transitions between an atomic condensate (AC), molecular condensate (M), and noncondensed atoms (EA) on forward (FW) and backward (BW) sweeps.

II. FORMATION OF A MOLECULAR CONDENSATE

Calculations were performed for two Na Feshbach resonances using values of parameters presented in Refs. [20,21]. The strong resonance, at 907 G, has the strength $\Delta=0.98$ G, and the weak one, at 853 G, has the strength $\Delta=9.5$ mG. The parameter values $\mu=3.65$ (in Bohr magnetons), $a_a=3.4$ nm, $\gamma=0.8\times10^{-10}$ cm^3/s, and $\gamma_m=10^{-9}$ cm^3/s are the same for both resonances. The neglect of elastic collisions is valid whenever $n_0(t_0)\ll10^{15}$ cm^{-3} for the weak resonance, and $n_0(t_0)\ll10^{17}$ cm^{-3} for the strong one. The spatial inhomogeneity can be neglected if the size of the condensate substantially exceeds $(8\times10^{-2}$ cm$^{-1/2})n_0^{-1/2}(t_0)$ and $(2.5\times10^{-2}$ cm$^{-1/2})n_0^{-1/2}(t_0)$, respectively, for the two resonances. Even when $n_0(t_0)=10^8$ cm^{-3}, these estimates set a minimal size of 8 μm for the weak resonance and 2.5 μm for the strong one. The variation of the magnetic field is considered linear in time, $B(t)=B_0+\dot{B}t$. The results are insensitive to the range of the magnetic-field variation whenever it exceeds $20gn_0^{1/2}/\mu$.

A relatively long-lived molecular condensate is formed more effectively in the case of a backward sweep, when the molecular state crosses the atomic one downwards (see Fig. 1), as proposed in Ref. [22]. (The resonance should be crossed upwards in advance, at a much higher ramp speed.) The maximal efficiency of conversion of the atomic condensate to a molecular one is $2\max(n_m)/n_0\approx0.8$ for the weak resonance [see Fig. 2(a)]. An increase of the atomic density, or a decrease of the ramp speed, should reduce the conversion efficiency due to inelastic collisions. On increase of the ramp speed, more atoms will be left in the atomic condensate (see Refs. [20,21]). At low atomic densities, the conversion becomes less efficient due to a temporary gain of population in the noncondensate atomic states. This observation is peculiar to, and emphasizes the importance of, the simultaneous consideration of inelastic collisions and molecular dissociation within the second-quantized approach.

Figure 3(a) shows that a substantial conversion efficiency is retained in both the weak and strong resonances in a wide range of the condensate density, leaving much freedom in the choice of the ramp speed appropriate for experiments. The

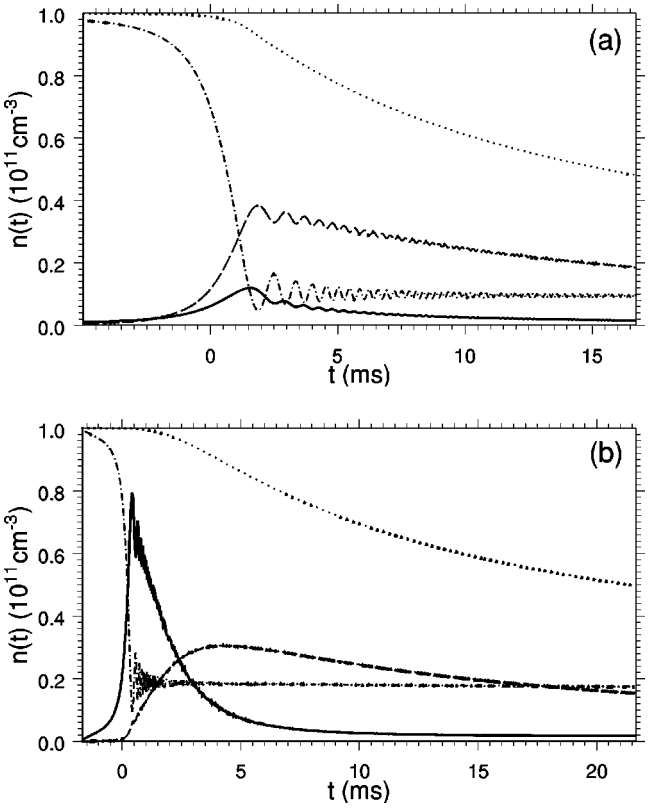

FIG. 2. Time dependence of the densities of the atomic condensate (dot-dashed line), the molecular condensate (dashed line), and the entangled atoms (solid line), calculated in a backward sweep with initial atomic density $n_0=10^{11}$ cm^{-3} for the weak resonance [the ramp speed $\dot{B}=-0.1$ G/s, (a)] and for the strong one [$\dot{B}=-20$ G/s, (b)]. The dotted line shows the total atomic density (sum of the atomic densities and twice the molecular one). The resonances are crossed at $t=0$.

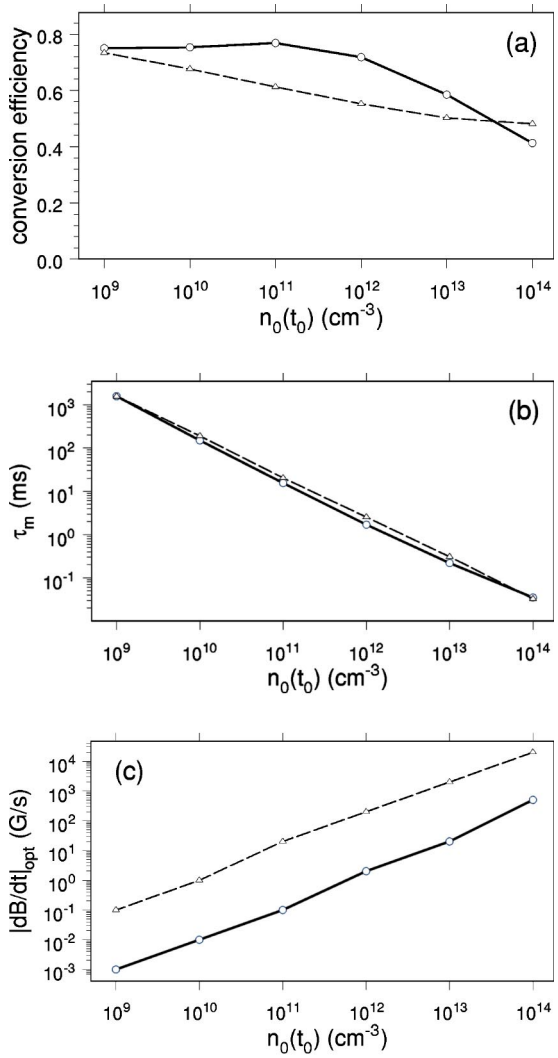

FIG. 3. Conversion efficiency (a), lifetime of the molecular condensate τ_m (b), and optimal ramp speed $\dot{B}_{\rm opt}$ (c), as a function of the initial atomic density calculated for the weak (solid line) and the strong (dashed line) resonances in a backward sweep.

lesser the initial density, the longer is the lifetime τ_m of the molecular condensate [see Fig. 3(b)], but the higher is the precision required for the control of the magnetic field.

The optimal ramp speed is approximately proportional to the initial density [see Fig. 3(c)]. This dependence minimizes the effect of a variation of parameters determining the conversion of the atomic condensate to the molecular one and the loss of molecular condensate. Indeed, the conversion to the molecular condensate is (in the fast decay approximation [20,21]) characterized by the parameter $g^2 n_0/\dot{B}$. Similarly, the loss is characterized by the ratio of the deactivation lifetime (which is inversely proportional to the initial density), and the crossing time (which is inversely proportional to the ramp speed).

Calculations for the strong Na resonance demonstrate a lower conversion efficiency [see Fig. 3(a)], due to a gain in the temporary formation of noncondensate atoms [cf. Figs. 2(a) and 2(b)]. The optimal ramp speed is about two orders of magnitude larger than in the weak resonance, given the same initial density [see Fig. 3(c)]. The use of the ^{85}Rb should be even less promising due to its high resonance strength $\Delta\approx 11$ G, in accordance with the low molecular population ($<3\%$) calculated in Ref. [24] pertaining to the recent JILA experiment [29].

III. FORMATION OF AN ENTANGLED GAS

The formation of noncondensate atoms due to Feshbach resonance has been recently observed in experiments [29] analyzed in Ref. [24]. As demonstrated in Ref. [13], these atoms are formed in squeezed states, which now turn out to be two-mode squeezed states, as in Ref. [7]. These states are similar to the state of electromagnetic radiation formed by parametric down-conversion (see Appendix D). As in quantum optics (see Ref. [2]), the amount of squeezing can be measured by the energy-dependent parameter $r(E,t)$ [see Eq. (E3) in Appendix E]. A mean-squeezing parameter, weighed by the spectral density of Eq. (16),

$$\overline{r}(t)=\int dE\tilde{n}_s(E,t)r(E,t)/n_s(t) \qquad (19)$$

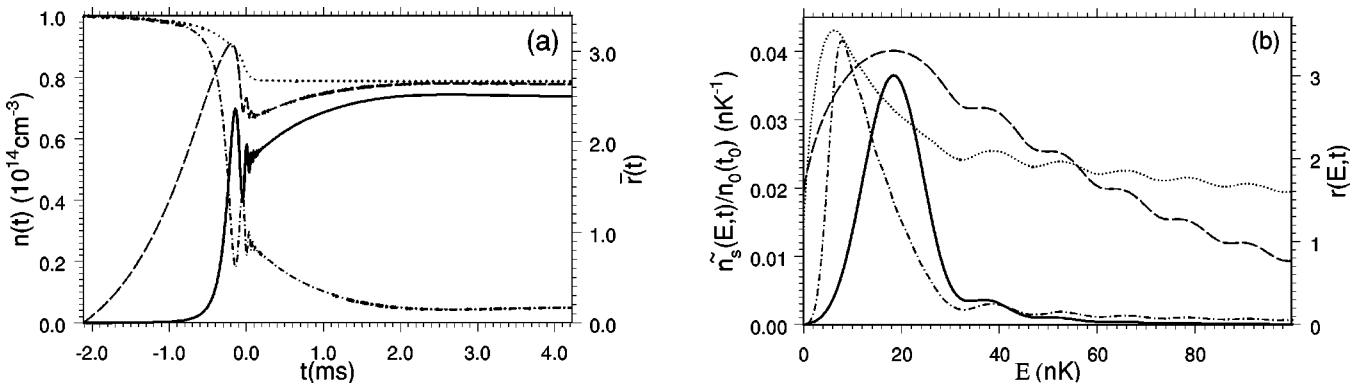

FIG. 4. (a) Time dependence of the densities of the atomic condensate (dot-dashed line), entangled atoms (solid line), and the total atomic density (dotted line) calculated for the weak resonance in Na with the initial atomic density $n_0=10^{14}$ cm^{-3} and ramp speed 50 G/s in a forward sweep. The dashed line shows the mean squeezing parameter $\bar{r}(t)$ [see Eq. (19)]. (b) Energy spectra of the entangled-atom density $\tilde{n}_s(E,t)$ (solid line) and the squeezing parameter $r(E,t)$ (dashed line) calculated at the peak, $t\approx -0.19$ ms. The dot-dashed and dotted lines show their values on the plateau at $t\approx 4$ ms.

is used to describe the time variation of the squeezing.

A stable gas of entangled atoms is formed by a forward sweep, in which the molecular state crosses the atomic one upwards (see Fig. 1). This process, too, is more efficient in the weak resonance. The molecular density is then very low and persists a shorter time (compared to that in the backward sweep) due to fast dissociation. Figure 4(a) demonstrates that more than 70% of the atomic condensate can be transformed into a gas of atoms in two-mode squeezed states with the mean-squeezing parameter $\bar{r}\approx 2.6$, corresponding to a noise reduction of about 23 dB. The time dependence of the mean squeezing has a peak of $\bar{r}\approx 3.1$ at $t\approx -0.19$ ms. The state of an entangled gas can be frozen at the peak time by fast turning off of the magnetic field. The energy spectra of the entangled-atom density and the squeezing parameter are presented in Fig. 4(b). The density spectra are rather narrow, and the peak energy increases with time. The squeezing parameter reaches the value of $r(E,t)\approx 3.5$ (corresponding to noise reduction of 30 dB) at the energy $E\approx 6$ nK and the time $t\approx 4$ ms.

CONCLUSIONS

Both quantum corrections and deactivating collisions are necessary for the analysis of molecular association in the atomic BEC due to Feshbach resonance in a time-dependent magnetic field. In a backward sweep, over 80% of the atomic population can be converted to a molecular condensate with lifetimes approaching 1 s. Low densities and narrow resonances are preferable for this purpose. The molecules dissociate onto atoms in two-mode squeezed states that are entangled. In a forward sweep, practically all atoms emerge in the entangled state with an unprecedented degree of squeezing, with the parameter r reaching a value of 3 and more.

APPENDIX A: DUMP STATE ELIMINATION

Second-quantized description of the atomic field requires a procedure for eliminating the dump state, different from the one used in Ref. [21]. It is similar to the Heisenberg-Langevin formalism of quantum optics (see Ref. [2]), but takes into account the nonlinearity of the collisional damping.

The Hamiltonian (1) yields the following equations of motion for the the annihilation operators $\hat{\Psi}_a(\mathbf{p},t)$ of the atomic field and $\hat{\Psi}_d(\mathbf{p},t)$ of the molecular dump states:

$$
\begin{aligned}
i\dot{\hat{\Psi}}_a(\mathbf{p},t)=&\left[\frac{p^2}{2m}+\epsilon_a(t)\right]\hat{\Psi}_a(\mathbf{p},t)+2(2\pi)^{-3/2}\\
&\times\int d^3p'\,V_h(\mathbf{p}-\mathbf{p}')\hat{\Psi}_a^{\dagger}(\mathbf{p}',t)\hat{\Psi}_m(\mathbf{p}+\mathbf{p}',t)\\
&+(2\pi)^{-3/2}\sum_d\int d^3p'\,d^3p_d d_d^*(\mathbf{p}_d-2\mathbf{p}')\\
&\times\hat{\Psi}_m^{\dagger}(\mathbf{p}'+\mathbf{p}_d-\mathbf{p},t)\hat{\Psi}_a(\mathbf{p}',t)\hat{\Psi}_d(\mathbf{p}_d,t)\\
&+(2\pi)^{-3/2}\sum_d\int d^3p_d d^3p_m d_d(\mathbf{p}_d-2\mathbf{p})\\
&\times\hat{\Psi}_d^{\dagger}(\mathbf{p}_d,t)\hat{\Psi}_m(\mathbf{p}_m,t)\hat{\Psi}_a(\mathbf{p}+\mathbf{p}_d-\mathbf{p}_m,t),
\end{aligned}
\tag{A1}
$$

$$
\begin{aligned}
i\dot{\hat{\Psi}}_d(\mathbf{p}_d,t)=&\left[\frac{p_d^2}{4m}-E_d\right]\hat{\Psi}_d(\mathbf{p}_d,t)+(2\pi)^{-3/2}\\
&\times\int d^3p'\,d^3p_m d_d(\mathbf{p}_d-2\mathbf{p}')\hat{\Psi}_a^{\dagger}(\mathbf{p}',t)\\
&\times\hat{\Psi}_m(\mathbf{p}_m,t)\hat{\Psi}_a(\mathbf{p}'+\mathbf{p}_d-\mathbf{p}_m,t)\\
&+(2\pi)^{-3/2}\sum_u\int d^3p_m d^3p_u d_{ud}(\mathbf{p}_u-\mathbf{p}_d)\\
&\times\hat{\Psi}_u^{\dagger}(\mathbf{p}_u,t)\hat{\Psi}_m(\mathbf{p}_m,t)\hat{\Psi}_m(\mathbf{p}_u+\mathbf{p}_d-\mathbf{p}_m,t).
\end{aligned}
\tag{A2}
$$

The atom and molecule emerging from the deactivation event (5) have momenta $p_d\geqslant P_d=\sqrt{4mE_d/3}$. The deactiva-

tion energy E_d substantially exceeds characteristic energies of atoms formed by dissociation of the condensate molecules, allowing us to discriminate two groups of atoms with momenta above and below $\min(P_d)$. Equations (A1) and (A2) give the following equations of motion for the product of the field operators [with $p_d \geqslant \min(P_d)$]:

$$i\frac{\partial}{\partial t}[\hat{\Psi}_d(\mathbf{p}_d,t)\hat{\Psi}_a(\mathbf{p}-\mathbf{p}_d,t)] \approx \left[\frac{p_d^2}{4m}+\frac{(\mathbf{p}_d-\mathbf{p})^2}{2m}-E_d\right]\hat{\Psi}_d(\mathbf{p}_d,t)\hat{\Psi}_a(\mathbf{p}-\mathbf{p}_d,t) + d_d(3\mathbf{p}_d-2\mathbf{p})\hat{\Psi}_a(\mathbf{p},t)\varphi_m(t), \tag{A3}$$

where ϵ_a is neglected as small compared to E_d, and the molecular field operator $\hat{\Psi}_m(\mathbf{p},t)$ is replaced by the mean field $\varphi_m(t)$ [see Eq. (9)]. The source term in Eq. (A3) arises from the commutation of field operators upon normal ordering, while the terms containing the dump field operators are neglected here. Substitution of the solution of Eq. (A3) and the molecular mean field (9) into Eq. (A1) gives the following integro-differential equation:

$$i\dot{\hat{\Psi}}_a(\mathbf{p},t)=\left[\frac{p^2}{2m}+\epsilon_a(t)\right]\hat{\Psi}_a(\mathbf{p},t)+2V_h^*(2p)\varphi_m(t) \times\hat{\Psi}_a^\dagger(-\mathbf{p},t)-i\varphi_m^*(t)\int_{t_0}^{t}K(t-t')\varphi_m(t') \times\hat{\Psi}_a(\mathbf{p},t')+i\hat{F}(\mathbf{p},t), \tag{A4}$$

with a kernel

$$K(t-t')=\sum_d\int d^3p_d|d_d(3\mathbf{p}_d-2\mathbf{p})|^2 \times\exp\left[-i\left(\frac{p_d^2}{4m}+\frac{(\mathbf{p}_d-\mathbf{p})^2}{2m}-E_d\right)(t-t')\right] \tag{A5}$$

and a quantum noise source

$$\hat{F}(\mathbf{p},t)=-i\varphi_m^*(t)\sum_d\int d^3p_d d_d^*(3\mathbf{p}_d-2\mathbf{p})\hat{\Psi}_d(\mathbf{p}_d,t_0) \times\hat{\Psi}_a(\mathbf{p}-\mathbf{p}_d,t_0)\exp\left[-i\left(\frac{p_d^2}{4m}+\frac{(\mathbf{p}_d-\mathbf{p})^2}{2m}-E_d\right) \times(t-t_0)\right]. \tag{A6}$$

As in the Heisenberg-Langevin formalism, commutators of the quantum noise are related to the kernel, except that here this relation involves averages of the commutators,

$$\langle\text{in}|[\hat{F}(\mathbf{p},t),\hat{F}^\dagger(\mathbf{p}',t')]|\text{in}\rangle = \varphi_m^*(t)\varphi_m(t')K(t-t')\delta(\mathbf{p}-\mathbf{p}'). \tag{A7}$$

APPENDIX B: GENERALIZED PARAMETRIC APPROXIMATION

In the generalized the parametric approximation [7,13] the atomic-field operator is written in the form of Eq. (12). Equation (14) as well as the functions $\psi_{c,s}(p,t)$ are independent of the $\mathbf{p}$ direction. The condition

$$|\psi_c(p,t)|^2-|\psi_s(p,t)|^2=1 \tag{B1}$$

also holds. Substitution of Eq. (12) into Eq. (10) gives

$$\hat{A}(\mathbf{p},t)=\hat{\Psi}_a(\mathbf{p},t_0)+\int_{t_0}^{t}\frac{dt_1}{C(t_1)}[\psi_c^*(p,t_1)\hat{F}(\mathbf{p},t_1) -\psi_s(p,t_1)\hat{F}^\dagger(-\mathbf{p},t_1)]. \tag{B2}$$

The representation of the field operator, given by Eqs. (12) and (B2), differs from the older parametric approximation [13] by the factor $C(t)$ in Eq. (12) and the second term, containing the quantum noise, in Eq. (B2). The factor $C(t)$ describes the decay due to deactivating collisions, while the quantum noise provides the correct commutation relations of the atomic-field operators (in the sense of averages) as

$$\langle\text{in}|[\hat{\Psi}_a(\mathbf{p},t),\hat{\Psi}_a^\dagger(\mathbf{p}',t)]|\text{in}\rangle=\delta(\mathbf{p}-\mathbf{p}'). \tag{B3}$$

Equations (12), (B2), and (11) lead to the following expressions for the two-atom correlation functions:

$$\langle\text{in}|\hat{\Psi}_a^\dagger(\mathbf{p},t)\hat{\Psi}_a(\mathbf{p}',t)|\text{in}\rangle=(2\pi)^3n_0(t)\delta(\mathbf{p})\delta(\mathbf{p}') +n_s(p,t)\delta(\mathbf{p}-\mathbf{p}'), \tag{B4}$$

$$\langle\text{in}|\hat{\Psi}_a(\mathbf{p},t)\hat{\Psi}_a(\mathbf{p}',t)|\text{in}\rangle=(2\pi)^3m_0(t)\delta(\mathbf{p})\delta(\mathbf{p}') +m_s(p,t)\delta(\mathbf{p}+\mathbf{p}'), \tag{B5}$$

where

$$n_0(t)=|\psi_c(0,t)\varphi_0+\psi_s(0,t)\varphi_0^*|^2C^2(t) \tag{B6}$$

is the condensate density,

$$n_s(p,t)=\{|\psi_s(p,t)|^2[1+\eta_s(p,t)]+|\psi_c(p,t)|^2\eta_s(p,t) -2\,\text{Re}[\psi_s^*(p,t)\psi_c(p,t)\eta_c(p,t)]\} \tag{B7}$$

is the momentum spectrum of the noncondensate atoms, and

$$m_0(t)=[\varphi_0\psi_c(0,t)+\varphi_0^*\psi_s(0,t)]^2C^2(t),$$

$$m_s(p,t)=\psi_s(p,t)\psi_c(p,t)[1+2\eta_s(p,t)]-\psi_c^2(p,t)\eta_c(p,t) -\psi_s^2(p,t)\eta_c^*(p,t) \tag{B8}$$

are the anomalous densities of the condensate and noncondensate atoms. The functions

$$\eta_s(p,t)=2\gamma C^2(t)\int_{t_0}^{t}\frac{dt'}{C^2(t')}|\varphi_m(t')\psi_s(p,t')|^2,$$

$$\eta_c(p,t)=2\gamma C^2(t)\int_{t_0}^{t}\frac{dt'}{C^2(t')}|\varphi_m(t')|^2\psi_s(p,t')\psi_c^*(p,t')$$

describe the contribution of quantum noise.

APPENDIX C: RELATION TO THE MEAN-FIELD APPROACH

In order to compare the present approach to the treatment of the multiple-crossing effect in Ref. [21], consider the system in a normalization box of volume $\mathcal{V}$. Due to the time variation of the magnetic field, the molecular state crosses $\nu_\epsilon\mu\dot{B}$ atomic states per unit time, where

$$\nu_\epsilon=\frac{\mathcal{V}}{4\pi^2}m^{3/2}\epsilon^{1/2} \tag{C1}$$

is the number of atomic states per unit of the energy ϵ of their relative motion. If the depletion of the molecular field during each crossing can be neglected, the crossings can be considered by using the theory of Ref. [13], according to which $\exp(2\pi\lambda)-1$ atoms are formed by each crossing, where

$$\lambda=\frac{8\pi|a_a|\Delta}{m|\dot{B}|}n_m \tag{C2}$$

and $n_m=|\varphi_m|^2$ is the molecular density.

Therefore, the loss rate of the molecular population is

$$\dot{N}_m=-\tfrac{1}{2}(1-e^{-2\pi\lambda})e^{2\pi\lambda}\nu_\epsilon|\mu\dot{B}|. \tag{C3}$$

If the molecular density is small enough, such that $\lambda\ll 1$, one obtains a loss rate of the molecular density

$$\dot{n}_m\approx-2|a_a\mu|\Delta\sqrt{m\epsilon}n_m, \tag{C4}$$

in full agreement with Eq. (50) in Ref. [21].

The multiple crossing approach of Ref. [21] is in good agreement with the more exact approach of the present paper only whenever (a) the variation of the molecular field during each crossing is negligible; and (b) $\lambda\ll 1$ and the quantum effect of Bose enhancement, described by the positive-exponential factor in Eq. (C3), is negligible (see Ref. [13]). These conditions are obeyed with the parameters used in the calculations of Ref. [21] for the Na resonances, the results of which are confirmed by using the present approach. However, at other conditions, the two methods give different results. Moreover, the method of Ref. [21] does not describe quantum properties of noncondensate atoms, such as entanglement and squeezing, as well as the formation of noncondensate atoms in a backward sweep.

APPENDIX D: ENTANGLEMENT

The dissociation of the molecular BEC forms entangled pairs of atoms with opposite momenta, as in the case of an unstable atomic BEC (see Ref. [7]). In order to clarify the nature of this entanglement, let us write out a pseudo-Hamiltonian

$$\hat{H}_a=\sum_{p_z>0}\hat{H}(\mathbf{p},t) \tag{D1}$$

that leads to equations of motion for the atomic field (10), expressed as a sum of contributions of different momentum modes in a normalization box,

$$\begin{aligned}\hat{H}_a(\mathbf{p},t)=&\left[\frac{p^2}{2m}+\epsilon_a(t)-i\gamma|\varphi_m(t)|^2\right][\hat{\Psi}_a^\dagger(\mathbf{p},t)\hat{\Psi}_a(\mathbf{p},t)\\&+\hat{\Psi}_a^\dagger(-\mathbf{p},t)\hat{\Psi}_a(-\mathbf{p},t)]\\&+\{2V_h(2p)\varphi_m^*(t)\hat{\Psi}_a(\mathbf{p},t)\hat{\Psi}_a(-\mathbf{p},t)+i\hat{F}(\mathbf{p},t)\\&\times[\hat{\Psi}_a^\dagger(\mathbf{p},t)+\hat{\Psi}_a^\dagger(-\mathbf{p},t)]+\text{H.c.}\}.\end{aligned} \tag{D2}$$

Although the pseudo-Hamiltonian is not hermitian, it allows writing the time evolution operator in the form

$$\hat{U}(t)=\prod_{p_z>0}\hat{U}(\mathbf{p},t), \tag{D3}$$

where (using the time-ordering operator T)

$$\hat{U}(\mathbf{p},t)=T\exp\left(-i\int_{t_0}^{t}\hat{H}_a(\mathbf{p},t')dt'\right). \tag{D4}$$

The representation of the operator $\hat{U}(t)$ as a product of single- mode operators $\hat{U}(\mathbf{p},t)$ follows from the commutativity of the $\hat{H}_a(\mathbf{p},t)$ with different values of $\mathbf{p}$.

Let us perform a measurement represented by a projection operator $\hat{P}(\mathbf{p})$, which selects atoms with the momentum $\mathbf{p}$ moving in the positive z direction, and does not affects atoms moving in the negative z direction. This measurement reduces the state vector $\hat{U}(t)|\text{in}\rangle$ to $\hat{P}(\mathbf{p})\hat{U}(t)|\text{in}\rangle=\hat{U}(\mathbf{p},t)|\text{in}\rangle$. The distribution of atoms moving in the negative z direction (the average number of atoms with the momentum, $\mathbf{p}',p_z'<0$), after this measurement will be determined by

$$\langle\text{in}|\hat{U}^\dagger(t)\hat{\Psi}_a^\dagger(\mathbf{p}',t)\hat{\Psi}_a(\mathbf{p}',t)\hat{U}(\mathbf{p},t)|\text{in}\rangle\propto\delta_{-\mathbf{pp}'}, \tag{D5}$$

representing an entanglement of atoms with opposite momenta. This analysis is similar to the one used in the entanglement of the signal and the idle in the process of degenerate two-photon down-conversion in quantum optics (see Ref. [2]).

APPENDIX E: SQUEEZING

As demonstrated in Ref. [13], the noncondensate atoms produced by molecular dissociation are formed in squeezed states, which now turn out to be two-mode squeezed states, as in Ref. [7]. As in quantum optics, the squeezing is related to the quadrature operators

$$\hat{X}(\mathbf{p},t)=\tfrac{1}{2}\{[\hat{\Psi}_a(\mathbf{p},t)\pm\hat{\Psi}_a(-\mathbf{p},t)]e^{i\theta} + [\hat{\Psi}_a^\dagger(\mathbf{p},t)\pm\hat{\Psi}_a^\dagger(-\mathbf{p},t)]e^{-i\theta}\}. \quad \text{(E1)}$$

The uncertainties of the quadratures can be written out as

$$\langle \text{in}|\hat{X}(\mathbf{p}_1,t)\hat{X}(\mathbf{p}_2,t)|\text{in}\rangle=\delta(\mathbf{p}_1-\mathbf{p}_2)\tfrac{1}{2}\{1+2n_s(p,t) \pm 2\,\text{Re}[m_s(p,t)e^{2i\theta}]\}, \quad \text{(E2)}$$

where the momentum spectra $n_s(p,t)$ and $m_s(p,t)$ are defined by Eqs. (B7) and (B8).

The uncertainties attain maximal and minimal values at two orthogonal values of the phase angle θ. The amount of squeezing can be measured by the parameter

$$r(\epsilon,t)=\frac{1}{4}\ln\frac{\langle \text{in}|\hat{X}(\mathbf{p}_1,t)\hat{X}(\mathbf{p}_2,t)|\text{in}\rangle_{\max}}{\langle \text{in}|\hat{X}(\mathbf{p}_1,t)\hat{X}(\mathbf{p}_2,t)|\text{in}\rangle_{\min}} =\frac{1}{4}\ln\frac{1+2n_s(p,t)+2|m_s(p,t)|}{|1+2n_s(p,t)-2|m_s(p,t)||}. \quad \text{(E3)}$$

[1] P. Meystre, *Atom Optics* (Springer, New York, 2001).
[2] M. O. Scully and M. S. Zubairy, *Quantum Optics* (Cambridge University Press, Cambridge, 1997).
[3] L. Deng *et al.*, Nature (London) **398**, 218 (1999); M. Trippenbach, Y.B. Band, and P.S. Julienne, Phys. Rev. A **62**, 023608 (2000); J.M. Vogels, K. Xu, and W. Ketterle, Phys. Rev. Lett. **89**, 020401 (2002).
[4] C. Orzel *et al.*, Science **291**, 2386 (2001).
[5] A. Sorenson, L.-M. Dian, J.I. Cirac, and P. Zoller, Nature (London) **408**, 63 (2001).
[6] J.A. Dunningham, K. Burnett, and M. Edwards, Phys. Rev. A **64**, 015601 (2001).
[7] V.A. Yurovsky, Phys. Rev. A **65**, 033605 (2002).
[8] D.C. Roberts, T. Gasenzer, and K. Burnett, J. Phys. B **35**, L113 (2002).
[9] J. Rogel-Salazar, S. Choi, G.H.C. New, and K. Burnett, Phys. Rev. A **65**, 023601 (2002).
[10] A.E.A. Koolen *et al.*, Phys. Rev. A **65**, 041601 (2002).
[11] U.V. Poulsen and K. Mølmer, Phys. Rev. A **63**, 023604 (2001).
[12] A. Vardi, V.A. Yurovsky, and J.R. Anglin, Phys. Rev. A **64**, 063611 (2001).
[13] V.A. Yurovsky, A. Ben-Reuven, and P.S. Julienne, Phys. Rev. A **65**, 043607 (2002).
[14] T. Opatrny and G. Kurizki, Phys. Rev. Lett. **86**, 3180 (2001).
[15] P.S. Julienne, K. Burnett, Y.B. Band, and W.C. Stwalley, Phys. Rev. A **58**, R797 (1998).
[16] E. Timmermans, P. Tommasini, M. Hussein, and A. Kerman, Phys. Rep. **315**, 199 (1999).
[17] R. Wynar *et al.*, Science **287**, 1016 (2000).
[18] J. Javanainen and M. Mackie, Phys. Rev. Lett. **88**, 090403 (2002).
[19] S. Inouye *et al.*, Nature (London) **392**, 151 (1998); J. Stenger *et al.*, Phys. Rev. Lett. **82**, 4569 (1999); S.L. Cornish *et al.*, *ibid.* **85**, 1795 (2000).
[20] V.A. Yurovsky, A. Ben-Reuven, P.S. Julienne, and C.J. Williams, Phys. Rev. A **60**, R765 (1999).
[21] V.A. Yurovsky, A. Ben-Reuven, P.S. Julienne, and C.J. Williams, Phys. Rev. A **62**, 043605 (2000).
[22] F.H. Mies, E. Tiesinga, and P.S. Julienne, Phys. Rev. A **61**, 022721 (2000).
[23] M. Holland, J. Park, and R. Walser, Phys. Rev. Lett. **86**, 1915 (2001).
[24] S.J.J.M.F. Kokkelmans and M.J. Holland, Phys. Rev. Lett. **89**, 180401 (2002).
[25] J.J. Hope, M.K. Olsen, and L.I. Plimak, Phys. Rev. A **63**, 043603 (2001); J.J. Hope, *ibid.* **64**, 053608 (2001); J.J. Hope and M.K. Olsen, Phys. Rev. Lett. **86**, 3220 (2001).
[26] K. Goral, M. Gajda, and K. Rzazewski, Phys. Rev. Lett. **86**, 1397 (2001).
[27] H.-Q. Zhou, J. Links, and R.H. McKenzie, e-print cond-mat/0207540.
[28] V.A. Yurovsky and A. Ben-Reuven, in *Spectral Line Shapes*, edited by Christina A. Back, AIP Conf. Proc. No. 645 (AIP, Melville, NY, 2002), Vol. 12, p. 479.
[29] E.A. Donley *et al.*, Nature (London) **417**, 529 (2002).